Cerebral Cortex June 2009;19:1330-1344
doi:10.1093/cercor/bhn171
Advance Access publication October 8, 2008

Interactions between Cortical Rhythms and Spiking Activity of Single Basal Ganglia Neurons in the Normal and Parkinsonian State

Plamen Gatev[1,3] and Thomas Wichmann[1,2]

[1]Yerkes National Primate Research Center, Emory University, Atlanta, GA 30329, USA and [2]Department of Neurology, School of Medicine, Emory University, Atlanta, GA 30322, USA
[3]Current address: Department of Cognitive Psychophysiology, Institute of Neurobiology, Bulgarian Academy of Sciences, 23 Acad. G. Bonchev Street, 1113 Sofia, Bulgaria.

In order to evaluate the specific interactions between cortical oscillations and basal ganglia–spiking activity under normal and parkinsonian conditions, we examined the relationship between frontal cortex electroencephalographic (EEG) signals and simultaneously recorded neuronal activity in the internal and external segments of the pallidum or the subthalamic nucleus (STN) in 3 rhesus monkeys. After we made recordings in the normal state, hemiparkinsonism was induced with intracarotid injections of the dopaminergic neurotoxin 1-methyl-4-phenyl-1,2,3,6-tetrahydropyridine (MPTP) in one animal, followed by additional recordings. Spiking activity in the pallidum and STN was associated with significant shifts in the level of EEG synchronization. We also found that the spectral power of beta- and gamma-band EEG rhythms covaried positively before the basal ganglia spikes but did not covary or covaried negatively thereafter. In parkinsonism, changes in cortical synchronization and phase coherence were reduced in EEG segments aligned to STN spikes, whereas both were increased in data segments aligned to pallidal spikes. Spiking-related changes in beta/gamma-band covariance were reduced. The findings indicate that basal ganglia and cortex interact in the processing of cortical rhythms that contain oscillations across a broad range of frequencies and that this interaction is severely disrupted in parkinsonism.

Keywords: EEG, globus pallidus, monkey, subthalamic nucleus, time-frequency analysis

Introduction

Basal ganglia, thalamus, and cortex are components of anatomical loops that are important in the control of motor and other functions. Functional abnormalities within these circuits may underlie some of the symptoms and signs of movement disorders, such as Parkinson's disease, or neuropsychiatric conditions, such as Tourette's syndrome (see, e.g., Saka and Graybiel 2003; DeLong and Wichmann 2007). Although the anatomy of the basal ganglia-thalamo-cortical circuits is known in considerable detail, our knowledge of the functional interactions between cortex and basal ganglia remains limited.

The available functional studies have investigated the interactions between the cerebral cortex and basal ganglia activity by combining electroencephalographic (EEG) recordings with either local field potential (LFP) recordings or recordings of single neuron–spiking activity in the basal ganglia. For instance, there have been several studies in which the relationship between basal ganglia LFPs and EEG activity were studied in parkinsonian patients with implanted deep brain stimulation (DBS) electrodes. In these studies, the implanted electrodes were used to record LFP signals in the subthalamic nucleus (STN) and in the internal segment of the globus pallidus (GPi). These studies demonstrated the existence of coherent beta-band activity between the LFPs in the STN and GPi and the concomitantly recorded EEG in unmedicated parkinsonian patients and a reduction of the beta-band activity when the patients underwent dopaminergic treatments (see reviews by Brown and Williams 2005; Gatev et al. 2006; Hammond et al. 2007). Based on these and other studies, models describing the normal function of the basal ganglia–cortical network have been developed in which basal ganglia activity serves to release cortical areas from "idling" alpha- and beta-band rhythms. The reduction of alpha- and beta-band activity allows oscillatory activities in the higher gamma range to manifest themselves. Such activities are considered to be important for active cognitive and other processes (Brown and Marsden 1998; Brown 2003). In frontal motor areas, switches between cortical activities in the alpha- and beta-band, and gamma-band oscillations may be necessary for the execution of sequential and other movements (e.g., Devos et al. 2003).

Other animal studies have examined the relationships between EEG signals and the electrical activities of single neurons in the basal ganglia in rats. Many of these experiments have been done under conditions in which the basal ganglia were the target of synchronous inputs (Steriade 2000; John et al. 2001; Imas et al. 2005; Massimini et al. 2005), such as during anesthesia in normal animals (Magill et al. 2000; Kasanetz et al. 2002), under dopamine-depleted conditions (Magill et al. 2001; Tseng et al. 2001; Belluscio et al. 2003; Walters et al. 2007), during episodes of sleep (Urbain et al. 2000; Mahon et al. 2006), or during wakefulness while the animals were displaying high-voltage spindle activity (in the 5–13 Hz range of frequencies, Berke et al. 2004; Dejean et al. 2007).

Studies of changes in the relationship between basal ganglia–spiking activity and cortical oscillations may provide us with a unique opportunity to bridge the gap that currently separates pathophysiologic models of the disease that are based on examinations of basal ganglia firing rates and patterns from those that are based on an assessment of LFP oscillations (see, for instance, Brown and Marsden 1998; Brown 2003; Gale et al. 2007). Some of the previous rodent studies have demonstrated the value of this approach (Urbain et al. 2000; Mahon et al. 2006). We here report on the result of a study of this kind in awake monkeys. We examined the interaction between cortical oscillatory activity and spike discharges of basal ganglia cells in the normal and parkinsonian states. We combined recordings of single-unit activities in STN, GPi, or the external pallidal segment (GPe) with EEG recordings from the primary motor cortex (MC) and the supplementary motor area (SMA).

Materials and Methods

Experimental Subjects

Three Rhesus monkeys (*Macaca mulatta*; 4–6 kg, 1 female and 2 males) were used for these studies. These animals had not been used for previous experiments and were sacrificed at the end of the studies described here. They were housed with ad libitum access to standard primate chow and water. Before any of the other procedures were carried out, the monkeys were trained to sit in a primate chair, to adapt to the laboratory and to permit handling by the experimenter. Throughout the experiments, adequate measures were taken to minimize pain or discomfort. All experimental protocols were performed in accordance with the National Institutes of Health "Guide for the Care and Use of Laboratory Animals" and the United States Public Health Service Policy on Humane Care and Use of Laboratory Animals (amended 2002) and were approved by the Animal Care and Use Committee of Emory University.

Surgical Procedures

Under general anesthesia with isoflurane gas (1–3%), 2 metal chambers were affixed to each animal's skull. The chambers were stereotactically directed at the pallidum or the STN on the animal's right side (for details, see Soares et al. 2004). During the same surgery session, each monkey was implanted with epidural Ag/AgCl pellet electrodes (diameter: 1 mm, length 2.5 mm; A-M Systems, Carlsborg, WA) over the SMA and MC, ipsilateral to the recording chambers. Each electrode was insulated and mounted in a short piece of stainless steel tubing that was inserted through a small hole drilled in the skull and secured in place with dental acrylic.

Electrooculography (EOG) electrodes, consisting of silver wire which was insulated up to the tip, were embedded in small skull openings drilled into the temporal corner and into the medial upper rim of the right orbit. EEG and EOG electrodes were connected to computer connectors which were also embedded in the acrylic cap. After completion of the recordings in the normal state, one of the male animals was rendered moderately hemiparkinsonian with 2 right-sided intracarotid injections with 1-methyl-4-phenyl-1,2,3,6-tetrahydropyridine (MPTP; injections separated by 2 weeks; total dose, 1.27 mg/kg). Stable parkinsonism was documented by weekly scoring of behavior (see detailed description of the behavioral methods in Soares et al. 2004). The post-MPTP recordings started 12 weeks after the second MPTP injection. At this time, the monkey showed obvious hypokinesia and bradykinesia of the arm and leg contralateral to the MPTP injections and a flexed posture of the arm but did not exhibit tremor. These symptoms corresponded to a level of 9 points on our 21-point parkinsonism rating scale which is based on 7 criteria (arm/leg bradykinesia, freezing, arm/leg posture, arm/leg tremor, amount of arm/leg movements, rigidity, and dystonia), each of which is rated on a scale of 0–3 (normal/absent to severe). There were no systematic changes in the rating scores between the beginning of the recordings and the time of sacrifice 16 weeks later. The animal did not receive any antiparkinsonian medications.

Neuronal Recordings

During the recording sessions, the animals were seated in a primate chair with their heads restrained. They did not perform specific tasks and did not receive rewards but they were permitted to move their trunk and limbs for small-amplitude postural adjustments and other movements. Throughout all experiments, observations of the monkey as well as electromyographic (EMG), EOG, and EEG recordings were used to judge the animal's state of wakefulness (see below). Neuronal recordings, cell identification, selection, and spike sorting were carried out with standard procedures as previously described (for details, see Soares et al. 2004). Neurons were recorded throughout the entire extent of STN, GPe, or GPi. Among GPe neurons, we restricted our analysis to the high-frequency discharge neurons, characterized by a regular firing pattern with pauses (see, e.g., DeLong 1971).

No attempts were made to restrict the recordings to specific functional territories within the basal ganglia nuclei. Previous anatomical studies have demonstrated that large portions of STN, GPe, and GPi are occupied by the "motor" circuitry of the basal ganglia, so that a large proportion of the recorded neurons is likely to have been related to motor functions. In the animal treated with MPTP, pre- and post-MPTP recordings were done in the same basal ganglia areas. The post-MPTP studies were carried out over a period of 16 weeks. Given the relatively small number of cells in which awake state recordings could be obtained for long enough periods of time (see below), we did not attempt to further classify the neurons according to their anatomic position within each nucleus.

The neuronal data along with the data on the timing of spike detection acceptance pulses were stored to computer disk for later analysis (MCP+, AlphaMap 4.8 datalogger, Alpha-Omega Engineering, Nazareth, Israel). The sampling rate of spike detection pulses was 12 kHz. Cells were recorded from for a minimum of 5 min, but most recordings were, in fact, 10 to 20 min long.

EEG, EMG, and EOG Recordings

We report here the results of bipolar EEG recordings from pairs of epidural Ag/AgCl electrodes, positioned over the animal's right SMA and MC, respectively, with 3- to 4-mm interelectrode distances ipsilateral to the neuronal recordings. The electrode impedance was less than 10 kΩ. EEG signals were filtered (0.16–70 Hz, no notch filter) and recorded with an 8-channel EEG amplifier (EEG-5208, Nihon-Kohden, Tokyo, Japan). These EEG filter settings were chosen because they represented the widest frequency range allowed by the EEG amplifiers. Voltage calibration was carried out on each recording day with 20-μV sinusoidal and rectangular pulses for each EEG channel.

Prior to each of the recording sessions, disposable electrodes for surface EMG were placed over the nuchal muscles (Nikomed, Doylestown, PA). EMG and EOG signals were filtered and amplified (amplifier model 1700, A-M Systems) using a frequency band between 10 Hz and 3 kHz for EMG data and between 1 and 100 Hz for EOG signals. EEG signals (digitized at 376 Hz), EMG signals (digitized at 12 kHz), and EOG signals (digitized at 376 Hz) were also stored to computer disk along with the simultaneously recorded neuronal signals.

Histology

At the termination of the study, the animals were sacrificed with an overdose of pentobarbital (100 mg/kg) followed by intracardiac perfusion with fixative (4% paraformaldehyde/0.1% glutaraldehyde). The brains were removed from the skull, blocked, cut in serial coronal sections, and stained with cresyl violet. The microelectrode penetrations left visible tracks (see examples in Supplementary Fig. S1) that helped us to confirm that the recordings were done in the correct nucleus.

Data Processing

General Approach

Our analysis approach was based on findings from previous studies which demonstrated that behavioral or cognitive events in motor and other tasks that almost certainly involve changes in cortical activity are often associated with increases or decreases of activity in basal ganglia cells in GPi, STN, or GPe (e.g., DeLong 1971; Crutcher and DeLong 1984; Wichmann et al. 1994; Abdullaev et al. 1998; Aldridge and Berridge 1998; Wichmann and Kliem 2004; Barnes et al. 2005; Darbaky et al. 2005; Turner and Anderson 2005; Gdowski et al. 2007; Pasquereau et al. 2007). We hypothesized that the interactions between the cerebral cortex and the basal ganglia under these task conditions are also present during the alert resting state (see also recent neuroimaging and EEG studies, Biswal et al. 1995; Raichle et al. 2001; Laufs et al. 2003; Mason et al. 2007; Seeley et al. 2007; Williamson 2007) and that they can be detected as momentary accelerations or decelerations in basal ganglia discharge. We therefore analyzed not only the relationship between EEG oscillations and random basal ganglia firing events but also the interactions between EEG oscillations and basal ganglia firing during periods of increases or decreases of the instantaneous discharge rate.

To accomplish this goal, data from each cell were split into short consecutive epochs, each containing the same number of spikes (see below and Table 2, row labeled "Segments/cell"). Within each epoch,

the shortest, the longest, and a random interspike intervals (ISIs) were selected. Random ISIs were selected from among all the ISI in the epoch. The resulting series of spike timing data were labeled as "Short," "Long," and "Rand" data. The relationship between EEG oscillations and the basal ganglia spiking events at the start or end of the chosen ISIs was assessed with spiking-related time-frequency, single-segment analysis of spectral power, and intersegment phase coherence (Pfurtscheller and Aranibar 1977; Tallon-Baudry et al. 1996; Delorme and Makeig 2004). Partial covariances of the average spectral power across the frequencies in the "sub-beta" (0.7–12.5 Hz), beta (13.2–30.1 Hz), and gamma bands of frequencies (30.8–69.7 Hz) were also calculated for the pre- and postspiking epochs. In addition, we calculated spike-triggered EEG averages for each of the data series. All analysis steps were carried out with Matlab (MathWorks, Natick, MA).

Comparison of ISI Data across Animals

In order to compare ISI data across animals (see Table 1), we statistically compared different descriptors of ISIs collected from STN, GPe, and GPi in the normal states (see also our previous papers, e.g., Soares et al. 2004; Kliem et al. 2007). For this analysis, the entire ISI stream from the different cells was used. In addition to the average ISI lengths, we examined the coefficient of variation (CV; calculated as the ratio of standard deviation and the mean ISI length) and calculated a "burst index." Bursts were detected with an algorithm developed by Legendy and Salcman (1985; Aldridge and Gilman 1991). This algorithm is based on the Poisson "surprise" method using a surprise value of 3 (see discussion in Wichmann and Soares 2006). The burst index was defined as the ratio between the number of spikes found in bursts and the total number of spikes. In addition, we analyzed the tendency of neurons to show oscillatory activity. As described in detail in our previous papers (Soares et al. 2004; Kliem et al. 2007), the ISI data were converted into frequencies and a power spectral analysis of the frequency representation (sampled at 200 Hz) was performed. We then integrated the neuronal power spectra in the sub-beta, beta-, and gamma-band (as defined above) and normalized each value to the total power in the sub-beta–gamma band range (Soares et al. 2004; Kliem et al. 2007).

Preprocessing of EEG Data

Consecutive data frames (each containing 10 s of simultaneously recorded EEG, EOG, EMG, and neuronal spike data) were inspected to exclude frames with signs of drowsiness (such as spindle activity, high-voltage delta activity, or evidence for rapid eye movement [REM] sleep). Frames with artifacts in the EEG traces caused by body or eye movements, scalp muscle activity, and other interferences were discarded. The remaining data frames were concatenated. EEG traces underwent 5-point median filtering for removal of high-frequency noise, linear detrending, and mean. Linear detrending across the whole frame and mean removal were done to eliminate small slow drifts (first-order or linear trends) and constant offsets (zero-order trends). This is an important preprocessing step in the time domain to remove nonstationarities and low-frequency variations without distorting the frequency and amplitude components of the periodicity being studied.

Selection of Spike Events

The ISI data set from single cells was divided into short consecutive epochs using the empirical formula $R = 0.5 \times W \times (\mathrm{FR} + 2 \times \mathrm{SD})$, where R is the number of spikes in the short epoch, W is the length of the segment evaluated with the time-frequency analysis in seconds (in this case 1.36 s), FR is the cell's overall mean firing rate in spikes per second, and SD is its standard deviation. In each case, R was rounded to the nearest whole number. The resulting epochs for individual cells contained the same number of spikes, but varied in duration, depending on the firing rates and their variations. We then identified the timing of the spike at the start of the shortest and longest ISIs in each epoch as well as the timing of the spike at the start of a randomly chosen ISI. All spikes in the epoch under study (including the shortest or longest) were eligible to be selected as a "random" ISI. These ISIs and the associated segments of EEG from MC or SMA constituted the Short, Long, and Rand data series.

The choice of the start or the end of an ISI as the alignment event in this analysis is arbitrary and would not be expected to affect the analysis of the Rand data series as any randomly chosen event would simply be preceded and followed by a similarly randomly chosen event. However, for the Short and Long ISI series, the choice of the alignment event is relevant. If individual ISIs are assumed to occur in random order (thus, neuronal firing can be described as a renewal process), a different alignment point (start vs. end of the ISI) would shift the spectral plots (or the plots of the coherence analyses) along the time axis by the mean ISI length. Alternatively, if the length of individual ISIs is in some way dependent on the length of preceding ISIs, the results would be more variable. In an analysis of the dependence of the spectral analysis on the choice of the alignment point, we found that moving the zero point from the start to the end of the index ISIs resulted in a (slight) shift of the peak of the spectrograms toward earlier time points (Supplementary Figs. S2 and S3). This finding was similar across the different data sets and is only shown for the STN data.

Analysis of the Relationship between EEG and Basal Ganglia–Spiking Events

The data were further processed with EEGLAB, an open source toolbox for analysis of single-segment EEG spectral dynamics (http://sccn.ucsd.edu/eeglab, see Makeig et al. 2004). EEGLAB's "timef" function was used to compute spiking-related changes in the EEG power spectrum for the time period between 512 ms before and 509 ms after the start of the respective Short, Long, or Rand ISIs based on Fourier transforms. We used 1.36-s data segments and a Hanning-tapered sliding time window (width 341 ms), repeatedly applying the Fourier transform across the segment in 2.7-ms steps with 4-fold oversampling and zero embedding. This procedure resulted in a final frequency resolution of 0.73 Hz across the range of frequencies from 0.37 to 70 Hz. The power spectra over the time windows were normalized for each frequency band to a segment baseline, which was calculated using a surrogate data distribution, constructed by selecting spectral estimates for each segment from randomly selected windows across the whole segment. The baseline was subtracted from the power values, and ratios between the residual and the baseline were

Table 1
Characteristic of inter-spike intervals (ISIs) from individual monkeys

	Monkey	Average ISI (ms)	CV	Firing rate (spikes/s)	Burst index (%)	Integrated power spectra (%)			*N*
						Sub-beta	Beta	Gamma	
GPe	U	23.1 ±11.2	1.5 ± 0.8	50.0 ± 16.5	20.0 ± 11.1	18.9 ± 2.9	21.6 ± 1.0	59.5 ± 3.1	18
	G	31.0 ± 11.0	2.1 ± 1.2	36.5 ± 12.9	29.4 ± 13.1	20.0 ± 3.8	21.2 ± 1.0	58.9 ± 4.0	50
	Y	28.7 ± 9.3	1.9 ± 1.0	38.1 ± 11.3	28.8 ± 9.9	20.7 ± 3.3	21.2 ± 1.0	58.3 ± 3.7	16
STN	U	57.6 ± 30.1	1.1 ± 0.3	20.3 ± 6.7	23.6 ± 1.9	17.3 ± 2.9	24.3 ± 1.4	58.4 ± 2.3	15
	G	72.0 ± 26.6	1.2 ± 0.1	15.4 ± 4.8	36.1 ± 9.7	20.7 ± 4.3	22.0 ± 1.3	57.3 ± 3.6	21
	Y	65.2 ± 9.2	1.4 ± 0.4	15.5 ± 2.1	27.6 ± 1.8	17.0 ± 1.4	23.0 ± 1.2	60.0 ± 0.6	3
GPi	U	19.6 ± 3.4	1.0 ± 0.2	52.2 ± 8.9	14.3 ± 3.8	17.1 ± 1.5	22.5 ± 1.0	60.4 ± 2.0	8
	G	25.0 ± 12.1	1.2 ± 0.4	45.1 ± 12.4	18.5 ± 10.8	16.9 ± 2.0	21.7 ± 1.0	61.4 ± 2.7	21
	Y	24.3 ± 6.8	1.0 ± 0.2	43.6 ± 9.8	16.0 ± 6.9	16.0 ± 2.7	21.2 ± 1.2	62.8 ± 3.6	10

Note: All entries, except for cell numbers, are means ± SD. ANOVA did not reveal significant differences between monkeys.

calculated. This resulted in normalized estimates of spiking-related changes of spectral power in the EEG signal over time for single segments. The single-segment estimates ($n > 128$ segments per cell) were subsequently averaged, first for individual cells and then across all cells within given data series. The program also provides the values of the spiking-related baseline spectral power for each of the studied frequencies.

To estimate the degree of phase locking between data segments, we measured the intersegment phase coherence ("phase-locking factor," Tallon-Baudry et al. 1996; Delorme and Makeig 2004). EEG spectral estimates at given frequencies and times are complex vectors in the 2-dimensional phase space where the norm and phase angle of each activity vector represent the amplitude and phase of the spectral estimate. To extract the phase information, we normalized the lengths of each of the segment activity vectors and then computed their complex average. After normalizing the amplitudes of the EEG spectral estimates, we determined the phase coherence between them and an event-phase indicator function (specific for each frequency and aligned to the spiking event) for each step of the sliding window. The resulting phase coherence values were averaged across segments for each cell.

Single-trial, time-frequency analysis is based on averaging the energy distribution of single EEG trials in the time-frequency plane. Contrary to averaging in the time domain, averaging in the time-frequency domain also identifies phenomena that are not connected with phase synchronization (Pfurtscheller and Lopes da Silva 1999; Tallon-Baudry and Bertrand 1999). This makes the method suitable for the evaluation of induced potentials, which are time-locked but not phase-locked. For comparison with the results of this analysis, we also calculated spiking-triggered EEG averages in the time domain, which evaluates the contribution of phase-locked response components. We calculated the mean of the normalized spike–triggered EEG averages and the 95% confidence intervals (CIs) for the Long, Short, and Rand series of data and identified the significance of peaks in the averages (Supplementary Figs. S12–S14). The normalization procedures avoid potential biases that might be caused by using absolute values from cells with "powerful" or "weak" modulation.

Spectral Analysis of Spontaneous EEG

To examine the overall impact of MPTP treatment on EEG, we calculated the spectral energy of the spontaneous EEG segments recorded from MC and SMA. We used the same EEG data as for the spiking-related time-frequency analysis (above), preprocessed, windowed, and oversampled in the same way. The average spectral energies were normalized and the power in each of the 95 frequency bands was expressed as a percentage of the total spectral power. We then averaged the resulting normalized EEG spectral energies from the normal cases and from the MPTP-treated cases and calculated 95% confidence limits. Next, the difference between the MPTP-treated state and the normal state was calculated with the 95% confidence limits for each band. We tested whether the averaged spectral energies differed significantly from each other using the data from those frequencies at which the differences between the spectral energies for the normal and MPTP-treated cases was greatest (2-tailed *t*-tests with Bonferroni–Holm adjustment).

Data Presentation and Statistics

Individual EEG spectral power values have a χ^2 distribution. Following the central limit theorem, averaging a large number of χ^2-distributed values (as done in our analyses) results in near-normally distributed means, so that parametric analyses can be applied (Kiebel et al. 2005).

Analyses of spiking-related changes in spectral power were done with different time and frequency resolutions. Figures 1, 3, and 5 show the highest resolution along both axes. For the data presentation in Figures 2, 4, and 6, we calculated the means of changes in overall spectral power at each time point across all 95 frequencies from 0.7 to 69.6 Hz (given the width of the individual frequency bands, the analysis covered the frequency range between 0.37 and 70 Hz), segments, and cells, with their 95% CIs for each of the data series.

For the presentation of data in Figure 7, we calculated the means and 95% CIs of the spiking-related baseline spectral power density across the population of cells available in each data set and compared the samples of differences for the 95 frequencies studied between pre- and postspiking-related means of spectral changes for the Short and Long series versus Rand series using Dunnett's 2-sided *t*-test. We also compared the data collected in the normal and MPTP states for each combination of basal ganglia and cortex structure with 2-tailed *t*-tests for independent samples (with Bonferroni–Holm adjustment for multiple comparisons). Differences between the Rand series and the Short or Long series for the MPTP data were evaluated as stated above.

To analyze the partial covariance between power spectral bands (Fig. 8), the frequency spectrum was split into 3 separate bands: the sub-beta band (0.7–12.5 Hz), the beta band (13.2–30.1 Hz), and the gamma band (30.8–69.6 Hz) and the means of spiking-related spectral changes in these bands were calculated across all cells for each basal ganglia and cortical structure in the 3 series (for a similar approach, see Priori et al. 2004). We evaluated the partial covariances separately for the data collected before and after the index events. Because these data were demeaned, we used the partial correlation procedure for this purpose. The coefficients of partial covariance were *Z* transformed and their difference from 0 was evaluated (1-tailed *t*-test, $P < 0.001$). A 1-way analysis if variance (ANOVA; Tukey's honest significant difference) was applied to evaluate the significance of the factor "pair of frequency bands" using the absolute values of differences between the *Z*-transformed coefficients for the pre- and postevent sections of the records of data collected in the normal state. To evaluate differences between measures obtained in the normal and parkinsonian states, we calculated the differences between the pre- and postspiking covariance coefficients for each cell and then used 2-tailed *t*-tests for independent samples (with Bonferroni–Holm correction). As above, we also compared these measures between the Rand and the Short or Long series of data in both states (Dunnett's *t*-test).

Maxima of the spiking-related baseline spectral power density for the whole range of frequencies were identified for each experimental group in averages calculated from all available cells and their values compared between the series of data collected in the normal and in the MPTP-treated state for the data presentation in Supplementary Figures S9–S11. The same was done specifically for the beta range of spiking-related baseline spectral power densities. The statistical tests were adjusted for multiple testing with the Bonferroni–Holm step-down procedure. Similarly, the differences between the SMA and MC regarding maxima in the whole spectra and in the beta range were tested for significance. Comparisons (Dunnett's *t*-test) between the Rand series and the Short or Long series of data did not produce significant results. For simplicity, we therefore present in Supplementary Figures S9–S11 only the Rand series of data.

Results

Characteristics of Neuronal Recording Data

There were no significant intersubject differences in terms of firing rates, burst indices, or integrated power spectra (Table 1). The data from all 3 monkeys were pooled for further analysis. The ISI lengths differed significantly between the Short, Long, and Rand groups of data in all structures ($P < 0.05$, Bonferroni–Holm adjusted, Table 2), whereas the averages of the ISIs in the Rand series were similar to those of the respective means calculated from the entire ISI streams (compare the first 2 rows shown in Table 2).

Comparisons of the data from the parkinsonian monkey to the data recorded in the normal state revealed that the average ISI length for GPe was longer in the parkinsonian state ($P < 0.05$, Bonferroni–Holm adjusted), whereas that from the STN was (nonsignificantly) shorter. These results are similar to previously reported findings, indicating that the average firing rate in GPe is reduced, whereas that in the STN is increased in parkinsonism (e.g., Bergman et al. 1994; Boraud et al. 2002). In all nuclei, the Short ISIs were shorter in the

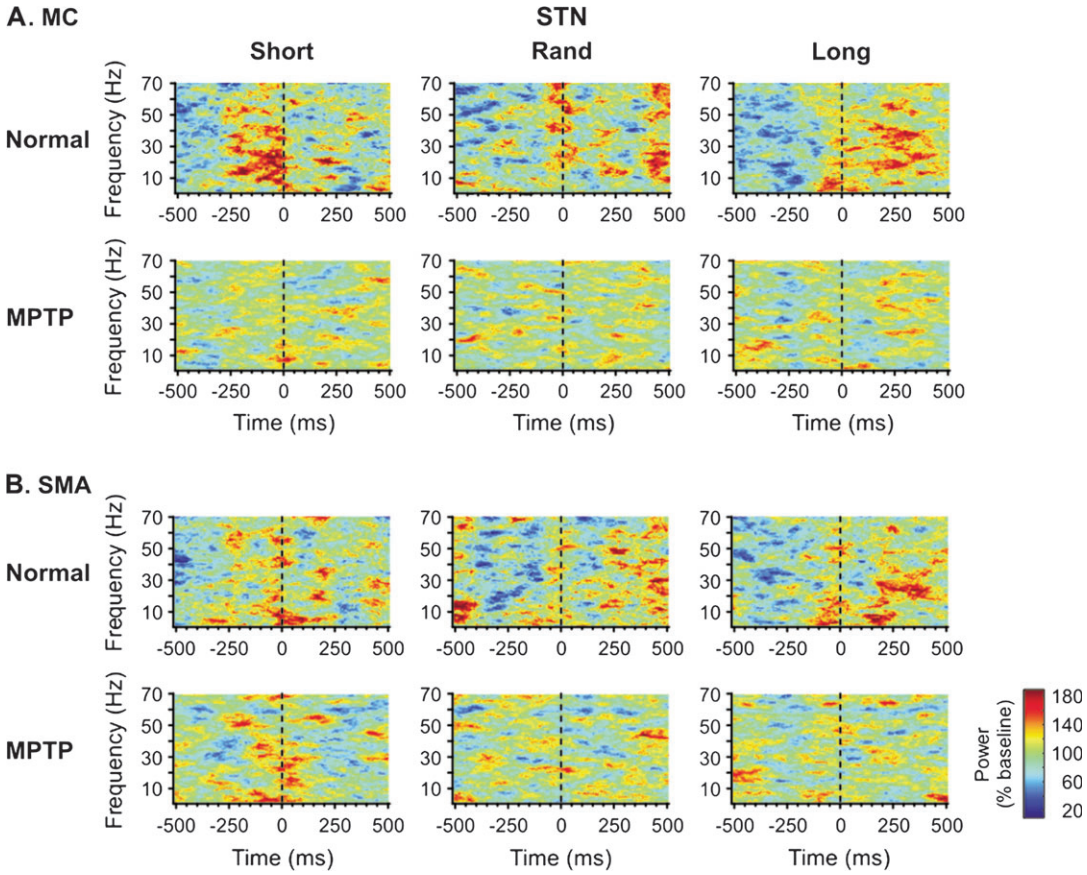

Figure 1. Single-segment, time-frequency analysis of spectral power changes in (*A*) MC- and (*B*) SMA-EEG related to single-cell spiking in the STN. These time-frequency maps are based on data pooled from all STN cells recorded in the normal state ($n = 39$ neurons) or in the parkinsonian state ($n = 36$). The data were normalized to the whole-segment baseline power (100%) and then averaged for each frequency across all available segments and cells. The *x*-axis shows time in milliseconds, the *y*-axis frequency in Hertz. Power values are color coded: green colors represent the whole-segment baseline, warmer colors indicate increases in spectral power, and cooler colors indicate decreases in spectral power. Time 0 is the onset of the chosen ISIs.

parkinsonian state than in the normal state (statistically significant only in the STN). At least in the STN, this may simply have been the result of an overall increase in firing rate because the average length of Long ISIs was also shortened. However, although Short ISIs do not necessarily correspond to bursts in discharge, it is likely that many short ISIs were, in fact, part of bursts. Parkinsonism is associated with significantly increased bursting throughout the basal ganglia (e.g., Wichmann and Soares 2006).

MPTP-Related Changes in Spontaneous EEG Spectral Power

MPTP treatment resulted in changed spectral power in MC- and SMA-EEG, affecting the sub-beta band in MC and SMA and the beta band in SMA. Details of this analysis are shown in Supplementary Figure S4. In both cortical structures, MPTP treatment resulted in a significant increase in spectral power at low frequencies (at 2.2 Hz in MC-EEG and 1.7 Hz in SMA-EEG) and a significant reduction at 6.6 Hz. In addition, power in the beta band was increased in the SMA-EEG (peak increase at 18.3 Hz). There was also a slight increase in the beta band in the MC-EEG after MPTP treatment. However, this did not reach significance. A significant reduction in spectral energy was seen in the spectra of the SMA-EEGs in the gamma band of frequencies (maximal change at 33 Hz).

Changes in the Spectral Power and Amplitude of EEG Related to Neuronal-Spiking Activity in the Basal Ganglia

EEG Changes Related to STN Spiking

There were obvious patterns in the EEG power spectra that were temporally related to the STN-spiking events in the normal state (Fig. 1, rows labeled "Normal"). For instance, the time-frequency maps for the Short and Long series differed substantially, particularly in the MC-EEG series of data (Fig. 1*A*). In the Short series, spectral EEG power was high across a broad range of frequencies before the basal ganglia spiking events and lower than the baseline thereafter. The opposite relationship was seen in the Long series. The Rand series of data represented an intermediate situation. Although qualitatively similar, the changes were quantitatively smaller in the SMA-EEG series compared with the MC-EEG series (Fig. 1*B*).

Figure 2 shows the time course of average spectral EEG power across the entire frequency range covered by our analysis (0.37–70 Hz) in relation to STN spiking. The average spectral power was increased immediately before the STN spikes (Fig. 2, rows labeled Normal). The prespike power increase was most substantial for the Short series of MC data. In the Long series, the postspike power was increased for several hundreds of milliseconds. These changes were more pronounced in the MC data than in the SMA data which were

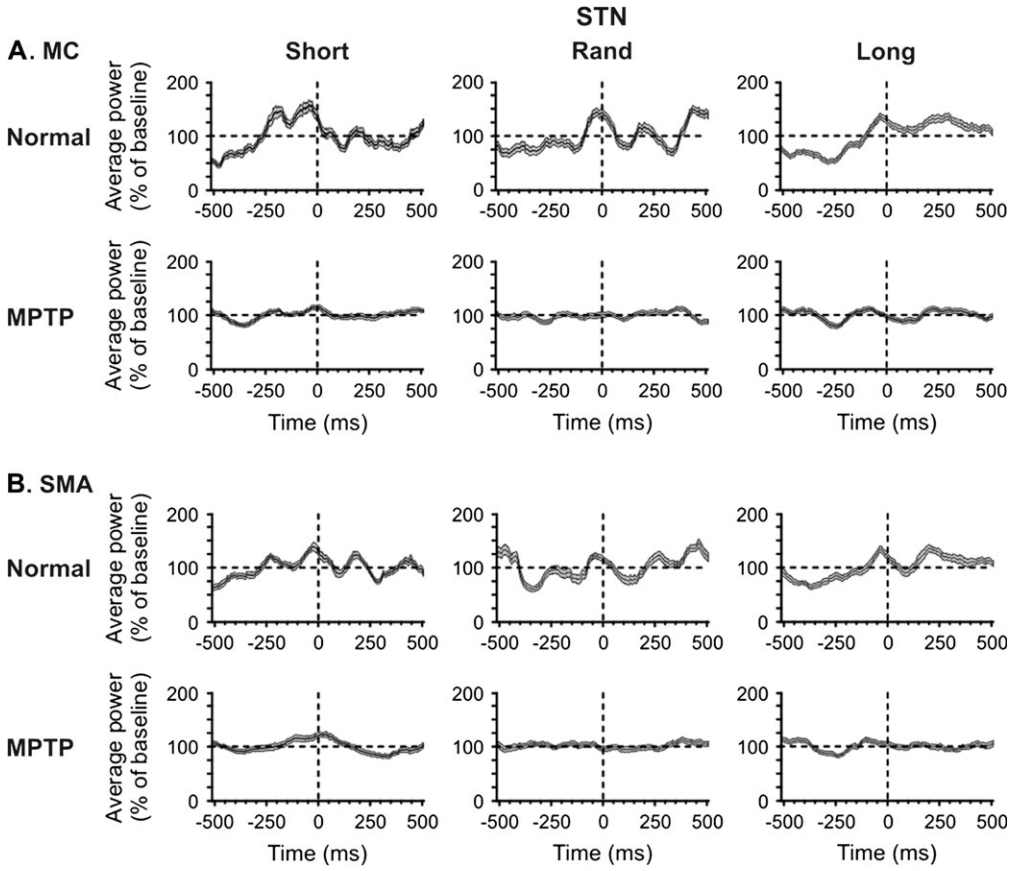

Figure 2. Mean spectral power of (*A*) MC- and (*B*) SMA-EEG related to STN spiking. In each case, the upper row of plots depict power averages based on data recorded in the normal state and the lower row of plots shows averages based on recordings in the MPTP-treated state. Numbers of cells are as stated in the legend to Figure 1. The gray areas around the mean lines are 95% CIs of the mean of the overall EEG spectral power.

Table 2
Characteristics of neuronal recording data

	STN		GPe		GPi	
	Normal	MPTP	Normal	MPTP	Normal	MPTP
Average ISI (ms)	65.9 ± 27.6	49.1 ± 20.1	28.8 ± 11.1	61.0 ± 80.2**	23.7 ± 9.7	25.2 ± 9.4
Rand ISI (ms)	66.1 ± 31.3	50.9 ± 18.1	28.7 ± 12.4	61.2 ± 82.5**	23.5 ±10.1	24.8 ± 9.0
Short ISI (ms)	28.1 ±16.1*	4.1 ± 1.8*,**	13.2 ± 8.8*	8.9 ± 17.8*	5.6 ± 3.9*	3.1 ± 0.84*,**
Long ISI (ms)	515 ± 273*	246.7 ± 83*,**	59 ± 162*	276.9 ± 168.6*	218 ± 148*	137.6 ± 51.6*,**
Segments/cell	199 ± 139	219 ± 133	205 ± 106	161 ± 79	181 ± 107	144 ± 56
Length of epochs (s)	1.74 ± 0.29	1. 65 ± 0.36	1.61 ± 0.35	1.48 ± 0.3	2.03 ± 0.31	1.79 ± 0.32
Number of cells	39 (15, 21, 3)	36 (36, 0, 0)	84 (18, 50, 16)	29 (29, 0, 0)	39 (8, 21, 10)	20 (20, 0, 0)

Note: All entries, except for the number of cells, are means ± SD. *$P < 0.05$, 2-tailed *t*-tests with Bonferroni–Holm correction, for comparisons against mean values calculated across the entire data epochs. **$P < 0.05$, 2-tailed *t*-tests with Bonferroni–Holm correction, for comparisons against corresponding values in normal monkeys. Brackets behind the total number of cells contain the number of cells from individual monkeys.

simultaneously recorded. The summary in Figure 7 (STN/Normal plots) shows the average total spectral power in the EEG signals for the entire extent of the pre- and postspike periods. For the Rand and Long series, the postspiking power was higher than the prespiking power, that is, a postspiking EEG synchronization was observed. Compared with the Rand series of data, the differences between pre- and postspike power were smaller for the Short series and greater for the Long series ("+" symbols, $P < 0.05$).

Treatment with MPTP substantially reduced the spiking-related changes in spectral power in the normal state (Figs. 1 and 2, rows labeled "MPTP"). The summary analysis (Fig. 7) showed that spiking-related shifts in spectral power in the EEGs decreased significantly after the MPTP treatment ("*" symbols, $P < 0.05$) in almost all series. After MPTP treatment, the Short and Long series were no longer significantly different from the Rand series.

EEG Changes Related to GPe Spiking

In EEG signals aligned to neuronal spiking in GPe under normal conditions, individual peaks in the time-frequency maps were lower than in the respective maps generated from EEG segments aligned to STN-spiking activity. In the Rand and Short series of data, spectral power was reduced postspiking (Figs. 3 and 4, rows

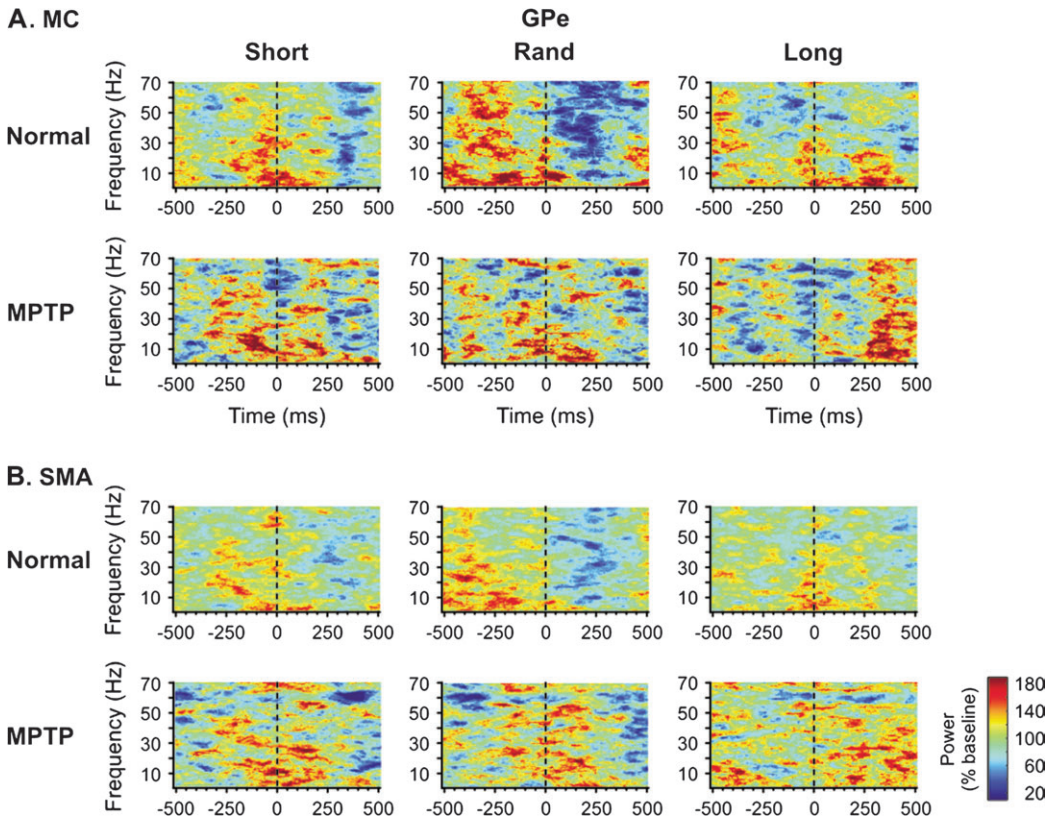

Figure 3. Single-segment, time-frequency analysis of spectral power changes in (*A*) MC- and (*B*) SMA-EEG related to single-cell spiking in the GPe. These time-frequency maps are based on data pooled from all GPe cells recorded in the normal state ($n = 84$) or in the parkinsonian state ($n = 29$). The format of the figure is similar to that of Figure 1.

labeled Normal). Spiking-related deviations from the baseline of the overall spectral power (averaged across the whole range from 0.37 to 70 Hz) were greater in the MC data (Fig. 3*A* and 4*A*, Normal) than in the SMA data (Fig. 4*B*, Normal) and the Rand series compared with the other 2 series. A peak of overall spectral power occurred just before or at the time of spiking. These peaks were followed by troughs (i.e., spiking-related desynchronization), 300–400 ms after spiking in the Short and Rand series of data. The summary analyses (Fig. 7, GPe/Normal plots) also show that the shifts between the spectral EEG power in the pre- and postspike epochs differed between the Rand series of data and the Short or Long series ($P < 0.05$). The postspike power averages were lower than the prespike averages in the Short and Rand series (i.e., spiking-related desynchronization was observed instead of synchronization).

In the MC Long series of data, MPTP treatment resulted in the appearance of a spectral power increase 250–500 ms after the index spikes (Figs. 3 and 4, rows of plots labeled MPTP), whereas reductions of the overall spiking-related mean power were seen in the other data series. The summary of pre- and postspike changes in spectral power (Fig. 7, GPe/MPTP plots) shows that the pre- and postspike differences in the Short and Rand series were smaller in the parkinsonian state than under control conditions ($P < 0.05$). However, in the Long series data sets from the MPTP-treated state, these differences increased compared with the normal state ($P < 0.05$), amounting to a sign reversal in this case.

EEG Changes Related to GPi Spiking

In the normal state, spiking-related increases in spectral power were seen before and around the time of the spiking events in the Short series of MC and SMA recordings, whereas the Long and Rand series showed smaller amounts of variation (Fig. 5, rows labeled Normal). The mean spectral power of spike-related EEG across the 0.3–70 Hz range reached a peak 150–200 ms before the spiking in the Short and Rand series (Fig. 6, rows labeled Normal). The summary analysis shown in Figure 7 (GPi/Normal) revealed that the prespike averages of spectral power were higher than the postspike averages in the Short and Rand series. The spectral power values were smaller in the Long than in the Short data series ($P < 0.05$).

The modulation of spectral EEG power in relation to GPi-spiking activity after MPTP treatment showed increased fluctuations in power, compared with the normal state (Figs. 5 and 6, rows labeled MPTP). The summary analysis of these changes (Fig. 7, GPi/MPTP) showed that the spiking-related pre- and postspike power shifts for the Short series were smaller than those seen in the normal state, whereas the shift in the Rand series was greater than that seen under normal conditions ($P < 0.05$).

Interband Partial Covariance of Spectral Power

To determine whether basal ganglia spiking is related to the correlation of oscillatory EEG power between distinct bands, we examined partial covariances of the mean spectral power across segments and cells in the sub-beta, beta, and gamma bands of frequencies before and after the spiking events. A significant positive partial covariance coefficient for a given pair of frequency bands indicates that power changes in the 2 bands increase or decrease together, whereas negative values

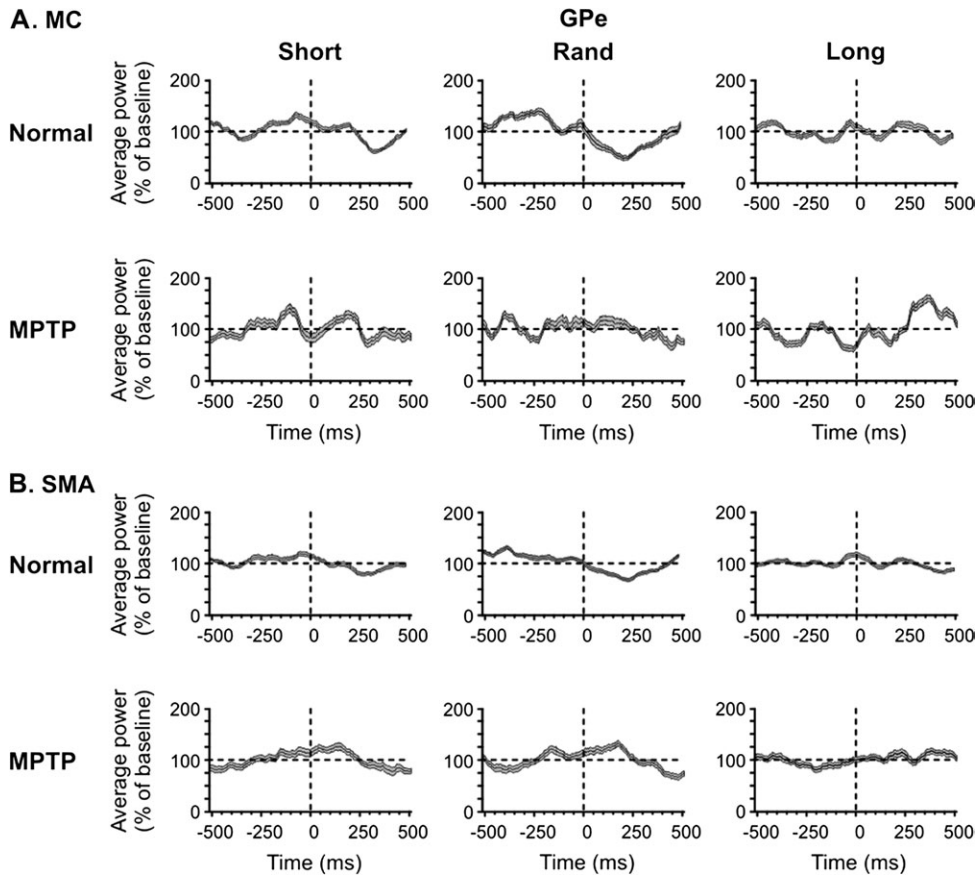

Figure 4. Mean spectral power of (*A*) MC- and (*B*) SMA-EEG related to GPe spiking. In each case, the upper row of plots depicts power averages based on data recorded in the normal state and the lower row shows averages based on data recorded in the MPTP-treated state. Numbers of cells are as stated in the legend to Figure 3. The format of the figure is similar to that of Figure 2.

indicate that an increase in one is accompanied by a decrease in the other.

One-way ANOVA revealed that the absolute values of differences of partial covariances between pre- and postevent periods were greater for the beta/gamma pair of frequency bands (n = 18, Z transformed r = 1.09 ± 0.52, mean ± SD) than for the sub-beta/beta-band and sub-beta/gamma pairs (n = 18, r = 0.63 ± 0.42 and 0.60 ± 0.54, respectively, $P < 0.05$, Tukey's honestly significant difference criterion). In the normal state, the prespiking beta/gamma partial covariances were significantly positive ($P < 0.001$) in all cases with the exception of the GPe/MC Long series. In all cases except for the GPi/SMA Rand series, the prespiking partial covariances were significantly higher than the postspiking partial covariances ($P < 0.05$), amounting to sign reversals in many of them (Fig. 8, rows labeled Normal).

The partial covariance data recorded in the parkinsonian state were significantly different from those recorded in the normal state (Fig. 8, rows labeled MPTP) but not consistent across the different series of data. In most of the MC-EEG series (Fig. 8*A*), the prespike partial beta/gamma-band covariance was reduced. In the GPe/MC Rand and Long series, the postspike partial beta/gamma-band covariance was more positive, whereas no change occurred in EEGs associated with GPi firing, and changes were mixed in the STN/MC series. The statistical comparisons of the differences between the pre- and postspike Z-transformed partial covariance coefficients showed in most MC cases a significant reduction in the parkinsonian state compared with the normal state ($P < 0.05$).

In the post-MPTP STN/SMA series of data, spiking was followed by an increase of the positive partial beta/gamma-band covariance, opposite to the changes seen under normal conditions. The pre- and postspiking partial beta/gamma-band covariance of SMA-EEG–related GPe and GPi spiking was variedly affected by the MPTP treatment.

In most cases, the differences between the pre- and postspike Z-transformed partial covariance coefficients were smaller in the parkinsonian state than in the normal state ($P < 0.05$).

Phase Coherence Analysis

The single-segment time-frequency analysis method allowed us to calculate intersegment phase coherence as a measure of phase locking of the basal ganglia spiking to the cortical oscillations between the EEG segments. This analysis demonstrated that for all cells and frequencies and across all conditions, the coefficients of phase coherence did not exceed 0.09 as a mean for each frequency across the whole epoch in population data. In comparison to the other series of data, the series triggered by STN spiking had the highest average phase coherence across frequencies (average phase coherence values of 0.07–0.09). As is shown in Supplementary Figures S5–S7 (rows labeled Normal), none of the data series recorded in the normal state showed evidence for specific peaks or troughs in the phase coherence plots in temporal association to basal ganglia spiking.

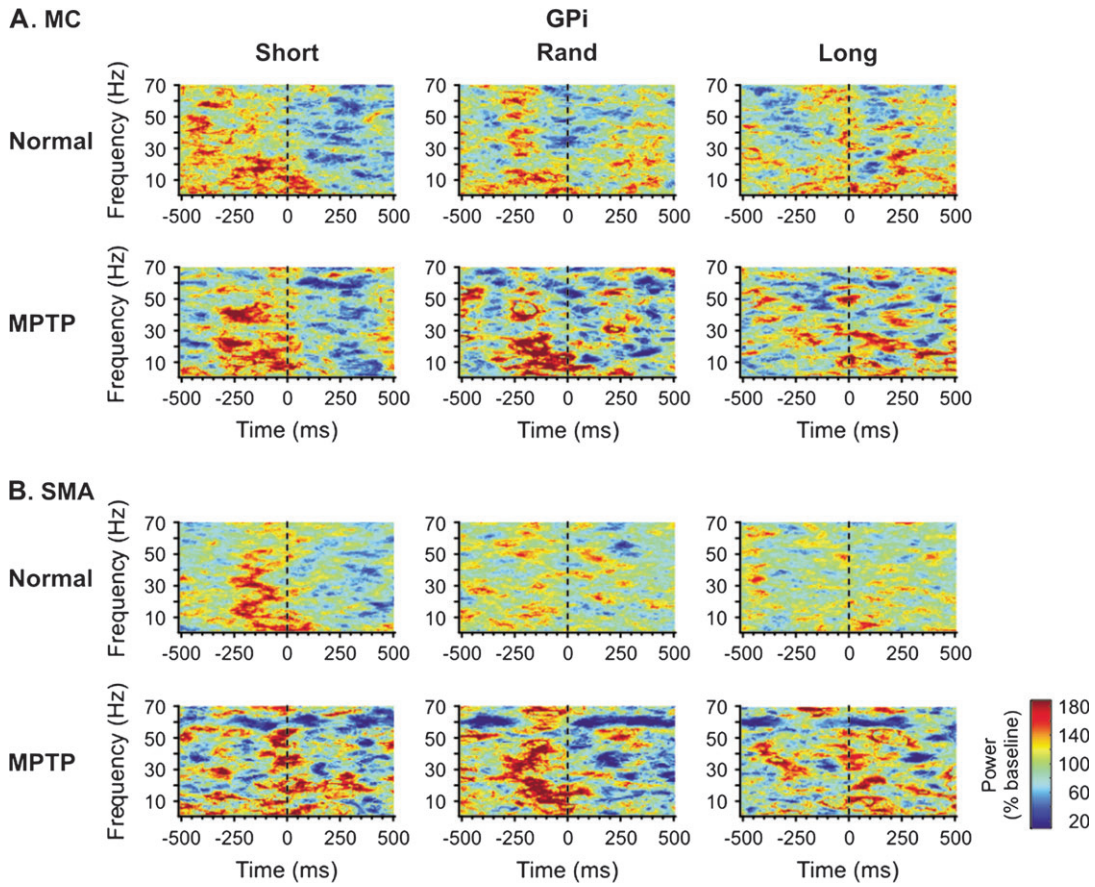

Figure 5. Single-segment, time-frequency analysis of spectral power changes in (*A*) MC- and (*B*) SMA-EEG related to single-cell spiking in the GPi. These time-frequency maps are based on data pooled from all GPi cells recorded in the normal state ($n = 39$) or in the parkinsonian state ($n = 20$). The format of the figure is similar to that of Figure 1.

In EEGs aligned to STN spiking in the post-MPTP phase of the experiment, the overall phase coherence was reduced compared with the normal state (Supplementary Figs. S5, rows labeled MPTP), whereas the phase coherence between EEG segments aligned to spiking activity in GPe or GPi was higher than in the normal state (Supplementary Figs. S6 and S7). In the STN spiking–related Short/SMA data series, there was an isolated peak in phase coherence in the beta range of frequencies around the time of the spiking events ($r = 0.135$; Supplementary Fig. S5B, MPTP). Beta range increases were also seen in some of the pallidal data series, but in that case, phase coherence also increased at higher frequencies.

A summary analysis of the average phase coherence data (expressed as the average phase coherence across the entire frequency range that was examined in this study analyzed separately for the pre- and postspike epochs) is shown in Supplementary Figure S8. The analysis confirmed that the intersegment phase coherence values were in general low. There were no differences between the pre- and postspiking intersegment phase coherence values in either the normal or the parkinsonian state. There were also no differences between the Short, Long, and Random data sets. Post-MPTP, the coherence values were generally lower in the data set based on STN data and higher in those based on GPi or GPe data ($P < 0.05$).

Analysis of Spiking-Related Baseline Spectral Energy

For all series, the maximum of the spiking-related spectral energy, averaged across cells and over the entire pre- and postspike epochs, was found between 3.7 and 3.9 Hz. This is shown for the Rand series of data in Supplementary Figures S9–S11. The Short and Long series of data were similar to the Rand series. There were no significant differences between the height of the spectral peaks in SMA or MC between the GPe, STN, and GPi series.

After MPTP treatment, significant changes were seen in the spectral power of EEG segments aligned to the spiking activity in STN or GPi. In these structures, the spectral peak in the SMA-EEG data was significantly larger than the peak in the MC data ($P < 0.05$). The beta-band spectral power was significantly higher in the post-MPTP series compared with the respective values in the normal state for the SMA data aligned to STN or GPi spiking (2-tailed *t*-test for the maximal values in the frequency range from 13.2 to 30.1 Hz, $P < 0.05$).

Analysis of Spike-Triggered Averages

Spike-triggered averaging of EEGs aligned to STN-spiking activity (Supplementary Fig. S12) showed small negative (i.e., upward) peaks around the time of spiking in the SMA-EEG in most cases. These did not (or only barely) reach significance. MPTP treatment did not induce significant changes except in the case of the Short/SMA series of data, which showed several small peaks before and after the spiking.

In the spike-triggered averages of EEG segments aligned to GPe firing (Supplementary Fig. S13), there were several small peaks at the time of spiking. The traces did not show any significant peaks after MPTP treatment.

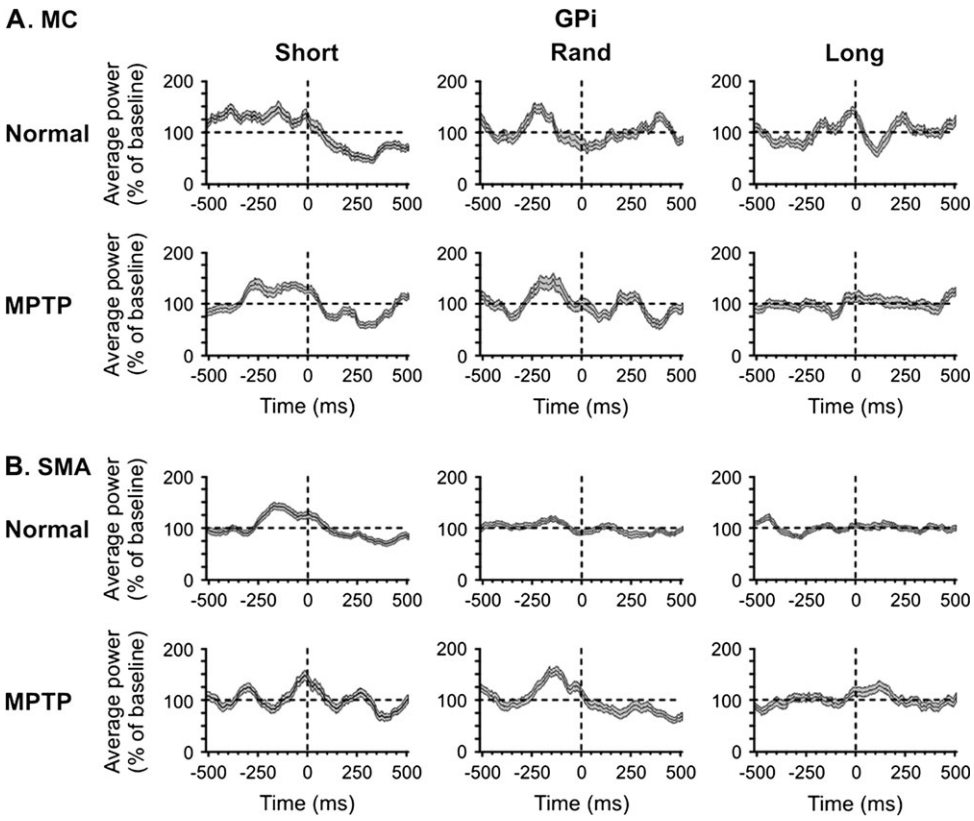

Figure 6. Mean spectral power of (*A*) MC- and (*B*) SMA-EEG related to GPi spiking. In each case, the upper row of plots depicts power averages based on data recorded in the normal state and the lower row shows averages based on data recorded in the MPTP-treated state. Numbers of cells are as stated in the legend to Figure 5. The format of the figure is similar to that of Figure 2.

Spike-triggered averaging analysis of EEG recorded together with GPi-spiking activity (Supplementary Fig. S14) did not show significant peaks in the normal state. In the parkinsonian state, there was a tendency toward increased fluctuation, specifically in the SMA-EEG series, where negative peaks were found after the spiking event. Except for the Rand series of data, these did not reach significance.

Discussion

The results show that spiking activity in GPe, STN, and GPi is associated with significant shifts in spectral power of cortical oscillatory activity in awake monkeys. Although these shifts do not follow a simple pattern, they are significantly different from baseline, raising the possibility that the interactions between basal ganglia–spiking activity and cortical rhythms are functionally relevant. This conclusion is also justified based on the partial covariance analysis, which revealed significant pre/postspiking shifts, particularly in the beta and gamma power covariance. We also found that the normal relationships between cortical and basal ganglia activity are strongly altered in the parkinsonian state together with changes in the spiking-related baseline spectral power and EEG phase coherence.

Short, Long, and Random ISIs

Short and Long ISIs correspond to momentary accelerations and decelerations of basal ganglia–spiking activity, respectively. Analyses based on the Rand series of data approximates an analysis in which all spikes would be included (see Table 2). We chose to analyze randomly selected spikes rather than all spikes in order to be able to directly compare the Rand series of data with the Short and Long series, each with identical numbers of segments per analysis.

The Short or Long ISIs were not related to specific behavioral phenomena. However, given previous findings indicating that behaviorally relevant events often induce changes in firing of basal ganglia neurons (see above), it is likely that many ISIs analyzed in the Short and Long series, in fact, reflected motor and/or sensory or cognitive changes that occurred under the "spontaneous" conditions tested here. It is also possible that the basal ganglia–thalamocortical system spontaneously transitions from a background state into states in which Short or Long ISIs occur. Regardless of the presence or absence of behavioral or cognitive changes triggering such transitions, we show that changes in basal ganglia firing are accompanied by characteristic changes in cortical oscillatory activity.

Basal Ganglia Spiking Is Related to Shifts in Cortical Synchronization and Interband Partial Covariance

We found that specific basal ganglia firing events in awake monkeys are related to transitions of cortical activity between episodes of increased and decreased spectral power, corresponding to periods of synchronization and desynchronization as well as transitions of the coupling between the beta- and gamma-frequency bands in cortical rhythms. The most straightforward interpretation of these findings is that oscillatory

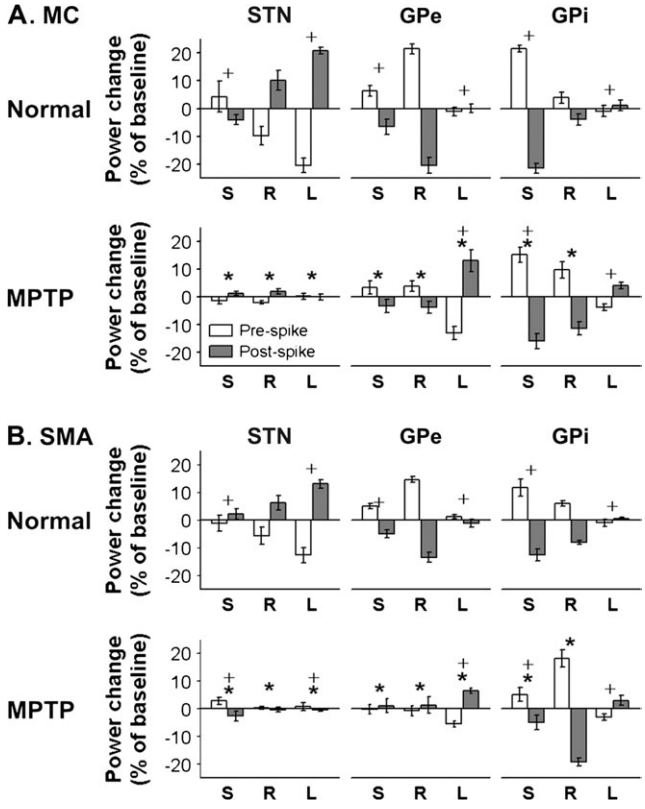

Figure 7. Spiking-related changes in spectral power of EEG in the normal and parkinsonian states. The figure shows averaged means of spectral power values of EEG from (*A*) MC and (*B*) SMA calculated for the periods before (open columns) and after (gray columns) the onset of the shortest (S), randomly chosen (R), or the longest (L) ISIs in short consecutive epochs of basal ganglia firing. Data were first normalized to the whole-segment background power and then averaged across all available EEG segments, frequencies, and cells from 3 monkeys for the normal state (upper row, labeled Normal) and from 1 monkey for the parkinsonian state (lower row, labeled MPTP). Error bars represent 95% CIs. Cases in which error bars do not cross the baseline (0%) are statistically different from the background ($P < 0.05$). $^{*}P < 0.05$, 2-tailed independent *t*-tests (Bonferroni–Holm adjusted), MPTP versus normal, of the mean of the differences between pre- and postspike power changes; $+P < 0.05$, 2-tailed paired Dunnett's *t*-tests for Short or Long versus Rand series, of the mean of the differences between pre- and postspike power changes, calculated separately for each combination of basal ganglia and cortex structure.

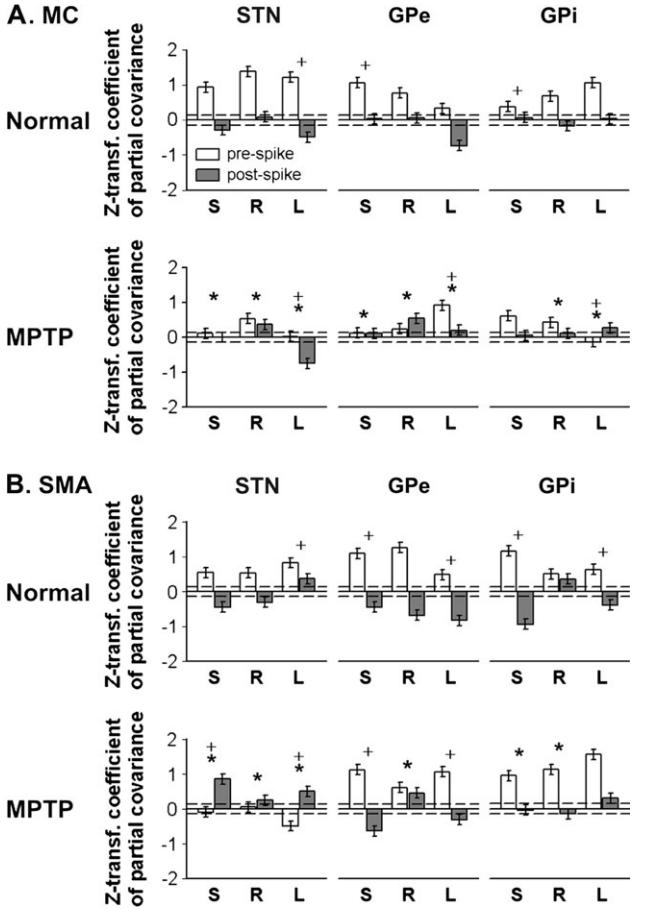

Figure 8. Spiking-related partial covariances between the spectral EEG power in the beta and gamma bands. The figure shows beta/gamma-band partial covariances for EEG data from (*A*) MC and (*B*) SMA calculated for periods before (open columns) and after (gray columns) the onset of the shortest (S), randomly chosen (R), or the longest (L) ISIs in short consecutive epochs of basal ganglia firing in 3 normal monkeys (upper row, labeled Normal) and in a parkinsonian monkey (lower row, labeled MPTP). Columns represent means ± 95% CIs of *Z*-transformed coefficients of partial covariance between beta and gamma bands, based on data averaged across respective frequencies, segments, and cells. Columns crossing the dashed lines indicate significant differences from zero ($P < 0.001$, 1-tailed *t*-test). $^{*}P < 0.05$, 2-tailed independent *t*-tests (Bonferroni–Holm adjusted), MPTP versus normal of the mean values across population cells of the differences between pre- and postspike *Z*-transformed covariance coefficients; $+P < 0.05$, 2-tailed independent Dunnett's *t*-tests, for Short or Long series versus Rand series of the mean values across population cells of the differences between pre- and postspike *Z*-transformed covariance coefficients, calculated separately for each combination of basal ganglia and cortex structure.

cortical activity influences the timing of firing in the basal ganglia and that basal ganglia–spiking activity, in turn, influences subsequent cortical oscillations. Our data do not allow us to directly distinguish this interpretation from the possibility that basal ganglia discharge simply reflects ongoing (independent) cortical activity. However, the fact that behavioral abnormalities result from focal basal ganglia pathology in diseases such as Parkinson's disease or hemiballismus and the fact that focal basal ganglia interventions, such as DBS, result in behavioral improvements in patients with movement disorders favor the view that basal ganglia activity does not merely reflect cortical activity but helps to shape it (Wichmann and DeLong 2006; DeLong and Wichmann 2007).

Power spectrum transitions in the EEG data were strongly dependent on the type of basal ganglia event to which they were correlated. Short and Long ISIs were often associated with different patterns of changes in EEG power, indicating that such events in basal ganglia firing are associated with different states of the basal ganglia–thalamocortical circuitry. In contrast, we found that the partial covariance between beta- and gamma-band activities in the EEG signals in the normal condition was generally more positive before the spiking events than after them, regardless of the ISI data series (for a similar analytical approach, see Priori et al. 2004). Thus, although shifts in synchronization patterns appear to be associated with specific types of basal ganglia events, the reduction in the positive beta/gamma partial covariance may be a general phenomenon associated with basal ganglia spiking per se, without consideration of specific firing patterns or dynamics beyond ISI lengths.

Basal ganglia–spiking activity was related to shifts in EEG synchronization at frequencies ranging across all frequency bands studied. Oscillations in these bands may have any of several different physiologic functions, which will be

considered in turn. One interpretation of the relationship between basal ganglia–spiking activity and oscillations in the EEG signals is that it may be involved in transitions between idling and more active states. Transient synchronization of EEG activity in the alpha and beta range, identified by spectral power increases in these bands, was proposed to represent cortex idling (Pfurtscheller and Lopes da Silva 1999; Devos et al. 2003), whereas desynchronization or reductions in spectral power in this range of frequencies may relate to transitions to a cortical state of active processing (Pfurtscheller and Aranibar 1977; Pfurtscheller and Lopes da Silva 1999). The traditional interpretation of alpha- and beta-band activity as an idling state (e.g., Pfurtscheller et al. 1996a, 1996b), however, has recently been challenged by the view that cortical alpha- and beta-band (idling) rhythms may, in fact, serve cognitive processes, such as linking perception to action (see, e.g., Basar et al. 1999; Basar, Basar-Eroglu, et al. 2001; Ozgoren et al. 2005; Pineda 2005) or being involved in movement planning (Donoghue et al. 1998; Rubino et al. 2006). Even oscillations in the sub-alpha range of frequencies are now considered to be involved in cortical processing in the awake state. For instance, distributed cortical theta rhythms may be important in functions such as response control (Basar, Schurmann, Sakowitz 2001; Knyazev 2007).

Although some of our results support the idea that specific basal ganglia spiking events are related to transitions between cortical idling and more active states (Brown and Marsden 1998), the reverse process, that is, shifts from states of spiking-related desynchronization to states of spiking-related synchronization also occurred (see, e.g., the EEG segments aligned to STN-spiking activity). It has been suggested that such transient synchronization, specifically in the beta-band of frequencies, may be important for the execution of sequences of movements (Devos et al. 2003). Execution of sequential movements is known to engage the SMA and other frontal areas (Tanji and Mushiake 1996) which project to the STN (Hartmann-von Monakow et al. 1978; Nambu et al. 1996, 1997; Takada et al. 2001).

A second interpretation of the relationship between basal ganglia–spiking activity and EEG relates to the strong temporal relationship between basal ganglia spiking and changes in EEG spectral power in the gamma range that was also apparent in our data. In many cortical areas, the gamma-band EEG rhythms have been discussed in the context of "binding" (Singer 1993), that is, a brain process that represents, across different cortical areas, the temporal correlation between external stimuli, or cognitive and motor aspects of behavior. This mechanism of integration of information may be relevant in perception (Singer 1993; Tallon-Baudry et al. 1996), voluntary movements (Farmer 1998), cognition (Herrmann et al. 2004), selective attention (Fries et al. 2001), and learning (Engel et al. 2001). The finding that basal ganglia spiking was related to changes in power in cortical gamma-band oscillations is compatible with the view that the interactions between cortex and basal ganglia contribute to aspects of binding.

Finally, based on the findings that basal ganglia spiking was, in fact, associated with changes in a wide range of cortical rhythms and with changes in interband partial covariances, it may be appropriate to discuss the relationship between basal ganglia activity and cortical oscillatory activity across a broader frequency spectrum. Recent studies have demonstrated that cortical oscillatory activities in different frequency bands are not mutually exclusive but often occur together in the form of "nested" or "complex" waves (Lisman and Idiart 1995; Lisman 2005; Steriade 2006) which may have a higher information content than their component rhythms (Lisman 2005). For instance, magnetoencephalographic studies have shown that alpha- and beta-band rhythms can be divided into 10- and 20-Hz components, which are separately related to sensory and motor events and may coalesce according to task conditions (Salmelin et al. 1995). Complex waves are thought to transmit coupled information from one cortical area to another (Basar, Basar-Eroglu, et al. 2001; Varela et al. 2001) and are considered to be metastable, that is, at a balance between stability and instability (Bressler and Tognoli 2006; Fingelkurts et al. 2006), to allow for rapid coupling and uncoupling processes that are needed for efficient use of the information contained in complex waves. As an example, behavioral programs in prefrontal and premotor cerebral cortical areas may be coded in complex waves that may then need to be split into their component frequencies before they can be used in frontal cortical areas related to motor execution (Niedermeyer et al. 1997). Our finding that basal ganglia firing is related to shifts in spectral patterns in the EEG and to changes in interband partial covariances suggests that the interaction between cortex and basal ganglia may serve to process and use the information that is carried by complex cortical waves, perhaps through assisting in uncoupling or recoupling of cortical processes.

Modulatory Nature of Interactions between Basal Ganglia and Cortex

Cortical input reaches STN, GPe, and GPi via several routes, including the monosynaptic corticosubthalamic route and bi- or polysynaptic pathways that pass through striatum or thalamus. Because of connections between STN, GPe, and GPi, all the 3 nuclei may receive cortical inputs by any or all of these routes. The functional balance between these pathways between the cerebral cortex and the basal ganglia has not been conclusively established, but it is clear that the transstriatal pathways (e.g., Pasupathy and Miller 2005; DeLong and Wichmann 2007) are anatomically more prominent than either the corticosubthalamic or the cortico-thalamo-basal ganglia projections. The known anatomy implies that all cortical input to GPe and GPi is at least bisynaptic, whereas a portion of cortical input to the STN is monosynaptic. Basal ganglia output reaches cortex via the thalamus (Crick and Koch 1998; Guillery and Sherman 2002; DeLong and Wichmann 2007). Feedback systems such as the thalamostriatal systems (Kimura et al. 2004; Smith et al. 2004) or loops involving the basal ganglia and the pedunculopontine nucleus (Mena-Segovia et al. 2004) influence these interactions. Taken together, these aspects of anatomy suggest that the interaction between the basal ganglia and cortex are largely indirect and may be modulatory in nature. Consistent with this notion are our findings of low intersegment-phase coherence. The data indicate that EEG segments aligned to basal ganglia spiking were phase coherent in less than 1% of the examined data segments (resulting in phase coherence values of less than 0.09). In line with these findings, our analysis of spike-triggered EEG averages showed few significant deviations from the zero line, confirming the absence of a clear phase relationship between cortical activity and basal ganglia spiking. Spectral changes in the EEG therefore appear to be time- but not phase-locked to basal ganglia–spiking activity (Tallon-Baudry et al. 1996; David et al. 2006). Recent modeling work has also arrived at the conclusion

that the basal ganglia modulate the attractor of cortical network activity rather than influence cortical activity directly (Djurfeldt et al. 2001). A plausible model for the function of the basal ganglia–cortical interaction is that basal ganglia firing may modulate the strength of intracortical connections (Pfurtscheller and Lopes da Silva 1999; Tallon-Baudry and Bertrand 1999; Guillery and Sherman 2002; David et al. 2006).

The time course of the interaction between basal ganglia and cortex is also compatible with this view. Simple mono- or bisynaptic interactions would clearly not be compatible with the timing of changes in cortical oscillations that are related to basal ganglia firing spanning several 100 ms epochs on either side of the trigger spikes. Such protracted interactions, however, are not entirely unexpected from the literature. For instance, electrical cortical stimulation is known to induce changes in basal ganglia activity that outlasts the cortical stimulus often by hundreds of milliseconds (e.g., Nambu et al. 2000, 2002; Kita et al. 2004).

The modulatory nature of the interaction between basal ganglia and cortex may be an essential feature of the operations of the corticosubcortical networks. Stronger or more direct basal ganglia–cortical interactions may have deleterious effects because they may lead to entrainment of the intracortical circuitry into uncontrolled and disruptive oscillations (Crick and Koch 1998), perhaps interfering with the temporal coordination of cortical circuits (Uhlhaas and Singer 2006) or with the metastability of cortical signals (Bressler and Tognoli 2006). Aberrant oscillatory activity or entrainment of cortical or thalamocortical circuits is suspected to occur in several diseases (Llinas et al. 1999, 2005; Leckman et al. 2006; Uhlhaas and Singer 2006) and participation of the basal ganglia in aberrant synchronized oscillatory activity within corticosubcortical networks has been directly demonstrated to occur in patients with parkinsonism (see below and, for instance, Brown 2003; Devos et al. 2003; Brown and Williams 2005).

Interactions between Cortex and Basal Ganglia in Parkinsonism

LFP and EEG recordings in untreated parkinsonian patients have suggested that poorly modulated beta-band oscillations dominate the electrical activities in cortex, STN, and GPi. Our analysis of MC- and SMA-EEG confirms the emergence of pathological sub-beta- and beta-band oscillations in the parkinsonian state (Supplementary Fig. S4). It has been shown that such pathological activities are ameliorated, and symptomatic improvements are effected, by dopaminergic drugs and DBS of the STN and GPi (Brown and Marsden 1999; Devos et al. 2002; Devos and Defebvre 2006; Jech et al. 2006). Our finding of increased phase coherence and baseline power in the beta band around the time of spiking events supports the notion that changes in beta-band oscillations are important in parkinsonism. However, the data also suggest that other qualitative and quantitative changes in the interactions between cortex and basal ganglia exist, including reductions in the phase-locking of STN spiking to EEG for frequencies outside of the beta-band, a virtual loss of spiking-related modulation of spectral power in the EEG in relation to STN spiking, significant quantitative and qualitative changes in the modulation of EEG spectral power related to pallidal spiking, and significant changes in the patterns of beta/gamma partial covariance.

Our data demonstrate that the temporal relationship of cortical oscillatory activity to basal ganglia–spiking activity is disturbed in parkinsonism, perhaps resulting in disruption of the normal metastability of cortical rhythms, mainly affecting the beta and gamma ranges. Similar disturbances of metastability have also been discussed in the context of other disorders, such as schizophrenia, opioid dependency, and major depression (Fingelkurts et al. 2005, 2006). The disruption of the processing of cortical oscillatory activities may contribute to the development and manifestation of parkinsonian signs.

Supplementary Material

Supplementary material can be found at: http://www.cercor.oxfordjournals.org/.

Funding

National Institutes of Health/National Institute of Neurological Disorders and Stroke grants (NS42250, NS540515, and NS54976 to T.W.); Yerkes National Primate Research Center grant (RR-000165).

Notes

The authors thank M.A. Kliem for expert technical assistance. *Conflict of Interest*: None declared.

Address correspondence to email: twichma@emory.edu.

References

Abdullaev YG, Bechtereva NP, Melnichuk KV. 1998. Neuronal activity of human caudate nucleus and prefrontal cortex in cognitive tasks. Behav Brain Res. 97:159–177.

Aldridge JW, Berridge KC. 1998. Coding of serial order by neostriatal neurons: a "natural action" approach to movement sequence. J Neurosci. 18:2777–2787.

Aldridge JW, Gilman S. 1991. The temporal structure of spike trains in the primate basal ganglia: afferent regulation of bursting demonstrated with precentral cerebral cortical ablation. Brain Res. 543:123–138.

Barnes TD, Kubota Y, Hu D, Jin DZ, Graybiel AM. 2005. Activity of striatal neurons reflects dynamic encoding and recoding of procedural memories. Nature. 437:1158–1161.

Basar E, Basar-Eroglu C, Karakas S, Schurmann M. 1999. Are cognitive processes manifested in event-related gamma, alpha, theta and delta oscillations in the EEG? Neurosci Lett. 259:165–168.

Basar E, Basar-Eroglu C, Karakas S, Schurmann M. 2001. Gamma, alpha, delta, and theta oscillations govern cognitive processes. Int J Psychophysiol. 39:241–248.

Basar E, Schurmann M, Sakowitz O. 2001. The selectively distributed theta system: functions. Int J Psychophysiol. 39:197–212.

Belluscio MA, Kasanetz F, Riquelme LA, Murer MG. 2003. Spreading of slow cortical rhythms to the basal ganglia output nuclei in rats with nigrostriatal lesions. Eur J Neurosci. 17:1046–1052.

Bergman H, Wichmann T, Karmon B, DeLong MR. 1994. The primate subthalamic nucleus II: Neuronal activity in the MPTP model of parkinsonism. J Neurophysiol. 72:507–520.

Berke JD, Okatan M, Skurski J, Eichenbaum HB. 2004. Oscillatory entrainment of striatal neurons in freely moving rats. Neuron. 43:883–896.

Biswal B, Yetkin FZ, Haughton VM, Hyde JS. 1995. Functional connectivity in the motor cortex of resting human brain using echo-planar MRI. Magn Reson Med. 34:537–541.

Boraud T, Bezard E, Bioulac B, Gross CE. 2002. From single extracellular unit recording in experimental and human Parkinsonism to the development of a functional concept of the role played by the basal ganglia in motor control. Prog Neurobiol. 66:265–283.

Bressler SL, Tognoli E. 2006. Operational principles of neurocognitive networks. Int J Psychophysiol. 60:139–148.

Brown P. 2003. Oscillatory nature of human basal ganglia activity: relationship to the pathophysiology of Parkinson's disease. Mov Disord. 18:357–363.
Brown P, Marsden CD. 1998. What do the basal ganglia do? Lancet. 351:1801–1804.
Brown P, Marsden CD. 1999. Bradykinesia and impairment of EEG desynchronization in Parkinson's disease. Mov Disord. 14:423–429.
Brown P, Williams D. 2005. Basal ganglia local field potential activity: character and functional significance in the human. Clin Neurophysiol. 116:2510–2519.
Crick F, Koch C. 1998. Constraints on cortical and thalamic projections: the no-strong-loops hypothesis. Nature. 391:245–250.
Crutcher MD, DeLong MR. 1984. Single cell studies of the primate putamen II: Relations to direction of movement and pattern of muscular activity. Exp Brain Res. 53:244–258.
Darbaky Y, Baunez C, Arecchi P, Legallet E, Apicella P. 2005. Reward-related neuronal activity in the subthalamic nucleus of the monkey. Neuroreport. 16:1241–1244.
David O, Kilner JM, Friston KJ. 2006. Mechanisms of evoked and induced responses in MEG/EEG. Neuroimage. 31:1580–1591.
Dejean C, Gross CE, Bioulac B, Boraud T. 2007. Synchronous high-voltage spindles in the cortex-basal ganglia network of awake and unrestrained rats. Eur J Neurosci. 25:772–784.
DeLong MR. 1971. Activity of pallidal neurons during movement. J Neurophysiol. 34:414–427.
DeLong MR, Wichmann T. 2007. Circuits and circuit disorders of the basal ganglia. Arch Neurol. 64:20–24.
Delorme A, Makeig S. 2004. EEGLAB: an open source toolbox for analysis of single-trial EEG dynamics including independent component analysis. J Neurosci Methods. 134:9–21.
Devos D, Defebvre L. 2006. Effect of deep brain stimulation and L-Dopa on electrocortical rhythms related to movement in Parkinson's disease. Prog Brain Res. 159:331–349.
Devos D, Derambure P, Bourriez JL, Cassim DF, Blond S, Guieu JD, Destee A, Defebvre L. 2002. Influence of internal globus pallidus stimulation on motor cortex activation pattern in Parkinson's disease. Clin Neurophysiol. 113:1110–1120.
Devos D, Labyt E, Derambure P, Bourriez JL, Cassim F, Guieu JD, Destee A, Defebvre L. 2003. Effect of L-Dopa on the pattern of movement-related (de)synchronisation in advanced Parkinson's disease. Neurophysiol Clin. 33:203–212.
Djurfeldt M, Ekeberg O, Graybiel AM. 2001. Cortex-basal ganglia interaction and attractor states. Neurocomputing. 38–40:573–579.
Donoghue JP, Sanes JN, Hatsopoulos NG, Gaal G. 1998. Neural discharge and local field potential oscillations in primate motor cortex during voluntary movements. J Neurophysiol. 79:159–173.
Engel AK, Fries P, Singer W. 2001. Dynamic predictions: oscillations and synchrony in top-down processing. Nat Rev Neurosci. 2:704–716.
Farmer SF. 1998. Rhythmicity, synchronization and binding in human and primate motor systems. J Physiol. 509(Pt 1):3–14.
Fingelkurts AA, Fingelkurts AA, Ermolaev VA, Kaplan AY. 2006. Stability, reliability and consistency of the compositions of brain oscillations. Int J Psychophysiol. 59:116–126.
Fingelkurts AA, Fingelkurts AA, Kahkonen S. 2005. Functional connectivity in the brain–is it an elusive concept? Neurosci Biobehav Rev. 28:827–836.
Fries P, Reynolds JH, Rorie AE, Desimone R. 2001. Modulation of oscillatory neuronal synchronization by selective visual attention. Science. 291:1560–1563.
Gale JT, Amirnovin R, Williams ZM, Flaherty AW, Eskandar EN. 2008. From symphony to cacophony: pathophysiology of the human basal ganglia in Parkinson disease. Neurosci Biobehav Rev. 32:378–387.
Gatev P, Darbin O, Wichmann T. 2006. Oscillations in the basal ganglia under normal conditions and in movement disorders. Mov Disord. 21:1566–1577.
Gdowski MJ, Miller LE, Bastianen CA, Nenonene EK, Houk JC. 2007. Signaling patterns of globus pallidus internal segment neurons during forearm rotation. Brain Res. 1155:56–69.
Guillery RW, Sherman SM. 2002. The thalamus as a monitor of motor outputs. Philos Trans R Soc Lond B. 357:1809–1821.
Hammond C, Bergman H, Brown P. 2007. Pathological synchronization in Parkinson's disease: networks, models and treatments. Trends Neurosci. 30:357–364.
Hartmann-von Monakow K, Akert K, Kunzle H. 1978. Projections of the precentral motor cortex and other cortical areas of the frontal lobe to the subthalamic nucleus in the monkey. Exp Brain Res. 33:395–403.
Herrmann CS, Munk MHJ, Engel AK. 2004. Cognitive functions of gamma-band activity: memory match and utilization. Trends Cogn Sci. 8:347–355.
Imas OA, Ropella KM, Ward BD, Wood JD, Hudetz AG. 2005. Volatile anesthetics disrupt frontal-posterior recurrent information transfer at gamma frequencies in rat. Neurosci Lett. 387:145–150.
Jech R, Ruzicka E, Urgosik D, Serranova T, Volfova M, Novakova O, Roth J, Dusek P, Mecir P. 2006. Deep brain stimulation of the subthalamic nucleus affects resting EEG and visual evoked potentials in Parkinson's disease. Clin Neurophysiol. 117: 1017–1028.
John ER, Prichep LS, Kox W, Valdes-Sosa P, Bosch-Bayard J, Aubert E, Tom M, diMichele F, Gugino LD. 2001. Invariant reversible QEEG effects of anesthetics. Conscious Cogn. 10:165–183.
Kasanetz F, Riquelme LA, Murer MG. 2002. Disruption of the two-state membrane potential of striatal neurones during cortical desynchronisation in anaesthetised rats. J Physiol. 543:577–589.
Kiebel SJ, Tallon-Baudry C, Friston KJ. 2005. Parametric analysis of oscillatory activity as measured with EEG/MEG. Hum Brain Mapp. 26:170–177.
Kimura M, Minamimoto T, Matsumoto N, Hori Y. 2004. Monitoring and switching of cortico-basal ganglia loop functions by the thalamo-striatal system. Neurosci Res. 48:355–360.
Kita H, Nambu A, Kaneda K, Tachibana Y, Takada M. 2004. Role of ionotropic glutamatergic and GABAergic inputs on the firing activity of neurons in the external pallidum in awake monkeys. J Neurophysiol. 92:3069–3084.
Kliem MA, Maidment NT, Ackerson LC, Chen S, Smith Y, Wichmann T. 2007. Activation of nigral and pallidal dopamine D1-like receptors modulates basal ganglia outflow in monkeys. J Neurophysiol. 89:1489–1500.
Knyazev GG. 2007. Motivation, emotion, and their inhibitory control mirrored in brain oscillations. Neurosci Biobehav Rev. 31: 377–395.
Laufs H, Krakow K, Sterzer P, Eger E, Beyerle A, Salek-Haddadi A, Kleinschmidt A. 2003. Electroencephalographic signatures of attentional and cognitive default modes in spontaneous brain activity fluctuations at rest. Proc Natl Acad Sci USA. 100:11053–11058.
Leckman JF, Vaccarino FM, Kalanithi PS, Rothenberger A. 2006. Annotation: Tourette syndrome: a relentless drumbeat–driven by misguided brain oscillations. J Child Psychol Psychiatry. 47:537–550.
Legendy CR, Salcman M. 1985. Bursts and recurrences of bursts in the spike trains of spontaneously active striate cortex neurons. J Neurophysiol. 53:926–939.
Lisman J. 2005. The theta/gamma discrete phase code occuring during the hippocampal phase precession may be a more general brain coding scheme. Hippocampus. 15:913–922.
Lisman JE, Idiart MAP. 1995. Storage of 7+/-2 short-term memories in oscillatory subcycles. Science. 267:1512–1515.
Llinas R, Urbano FJ, Leznik E, Ramirez RR, van Marle HJF. 2005. Rhythmic and dysrhythmic thalamocortical dynamics: GABA systems and the edge effect. Trends Neurosci. 28:325–333.
Llinas RR, Ribary U, Jeanmonod D, Kronberg E, Mitra PP. 1999. Thalamocortical dysrhythmia: a neurological and neuropsychiatric syndrome characterized by magnetoencephalography. Proc Natl Acad Sci USA. 96:15222–15227.
Magill PJ, Bolam JP, Bevan MD. 2000. Relationship of activity in the subthalamic nucleus-globus pallidus network to cortical electroencephalogram. J Neurosci. 20:820–833.
Magill PJ, Bolam JP, Bevan MD. 2001. Dopamine regulates the impact of the cerebral cortex on the subthalamic nucleus-globus pallidus network. Neuroscience. 106:313–330.

Mahon S, Vautrelle N, Pezard L, Slaght SJ, Deniau JM, Chouvet G, Charpier S. 2006. Distinct patterns of striatal medium spiny neuron activity during the natural sleep-wake cycle. J Neurosci. 26:12587–12595.

Makeig S, Debener S, Onton J, Delorme A. 2004. Mining event-related brain dynamics. Trends Cogn Sci. 8:204–210.

Mason MF, Norton MI, Van Horn JD, Wegner DM, Grafton ST, Macrae CN. 2007. Wandering minds: the default network and stimulus-independent thought. Science. 315:393–395.

Massimini M, Ferrarelli F, Huber R, Esser SK, Singh H, Tononi G. 2005. Breakdown of cortical effective connectivity during sleep. Science. 309:2228–2232.

Mena-Segovia J, Bolam JP, Magill PJ. 2004. Pedunculopontine nucleus and basal ganglia: distant relatives or part of the same family? Trends Neurosci. 27:585–588.

Nambu A, Kaneda K, Tokuno H, Takada M. 2002. Organization of corticostriatal motor inputs in monkey putamen. J Neurophysiol. 88:1830–1842.

Nambu A, Takada M, Inase M, Tokuno H. 1996. Dual somatotopical representations in the primate subthalamic nucleus: evidence for ordered but reversed body-map transformations from the primary motor cortex and the supplementary motor area. J Neurosci. 16:2671–2683.

Nambu A, Tokuno H, Hamada I, Kita H, Imanishi M, Akazawa T, Ikeuchi Y, Hasegawa N. 2000. Excitatory cortical inputs to pallidal neurons via the subthalamic nucleus in the monkey. J Neurophysiol. 84:289–300.

Nambu A, Tokuno H, Inase M, Takada M. 1997. Corticosubthalamic input zones from forelimb representations of the dorsal and ventral divisions of the premotor cortex in the macaque monkey: comparison with the input zones from the primary motor cortex and the supplementary motor area. Neurosci Lett. 239:13–16.

Niedermeyer E, Naidu SB, Plate C. 1997. Unusual EEG theta rhythms over central region in Rett syndrome: considerations of the underlying dysfunction. Clin Electroencephalogr. 28:36–43.

Ozgoren M, Basar-Eroglu C, Basar E. 2005. Beta oscillations in face recognition. Int J Psychophysiol. 55:51–59.

Pasquereau B, Nadjar A, Arkadir D, Bezard E, Goillandeau M, Bioulac B, Gross CE, Boraud T. 2007. Shaping of motor responses by incentive values through the basal ganglia. J Neurosci. 27:1176–1183.

Pasupathy A, Miller EK. 2005. Different time courses of learning-related activity in the prefrontal cortex and striatum. Nature. 433:873–876.

Pfurtscheller G, Aranibar A. 1977. Event-related cortical desynchronization detected by power measurements of scalp EEG. Electroenceph Clin Neurophysiol. 42:817–826.

Pfurtscheller G, Lopes da Silva FH. 1999. Event-related EEG/MEG synchronization and desynchronization: basic principles. Clin Neurophysiol. 110:1842–1857.

Pfurtscheller G, Stancak A, Jr., Neuper C. 1996a. Event-related synchronization (ERS) in the alpha band—an electrophysiological correlate of cortical idling: a review. Int J Psychophysiol. 24:39–46.

Pfurtscheller G, Stancak A, Jr., Neuper C. 1996b. Post-movement beta synchronization. A correlate of an idling motor area? Electroencephalogr Clin Neurophysiol. 98:281–293.

Pineda JA. 2005. The functional significance of mu rhythms: translating "seeing" and "hearing" into "doing". Brain Res Rev. 50:57–68.

Priori A, Foffani G, Pesenti A, Tamma F, Bianchi AM, Pellegrini M, Locatelli M, Moxon KA, Villani RM. 2004. Rhythm-specific pharmacological modulation of subthalamic activity in Parkinson's disease. Exp Neurol. 189:369–379.

Raichle ME, MacLeod AM, Snyder AZ, Powers WJ, Gusnard DA, Shulman GL. 2001. A default mode of brain function. Proc Natl Acad Sci USA. 98:676–682.

Rubino D, Robbins KA, Hatsopoulos NG. 2006. Propagating waves mediate information transfer in the motor cortex. Nat Neurosci.

Saka E, Graybiel AM. 2003. Pathophysiology of Tourette's syndrome: striatal pathways revisited. Brain Dev. 25(Suppl 1):S15–S19.

Salmelin R, Hamaalainen M, Kajola M, Hari R. 1995. Functional segregation of movement-related rhythmic activity in the human brain. Neuroimage. 2:237–243.

Seeley WW, Menon V, Schatzberg AF, Keller J, Glover GH, Kenna H, Reiss AL, Greicius MD. 2007. Dissociable intrinsic connectivity networks for salience processing and executive control. J Neurosci. 27:2349–2356.

Singer W. 1993. Synchronization of cortical activity and its putative role in information processing and learning. Annu Rev Physiol. 55:349–374.

Smith Y, Raju DV, Pare JF, Sidibe M. 2004. The thalamostriatal system: a highly specific network of the basal ganglia circuitry. Trends Neurosci. 27:520–527.

Soares J, Kliem MA, Betarbet R, Greenamyre JT, Yamamoto B, Wichmann T. 2004. Role of external pallidal segment in primate parkinsonism: comparison of the effects of MPTP-induced parkinsonism and lesions of the external pallidal segment. J Neurosci. 24:6417–6426.

Steriade M. 2000. Corticothalamic resonance, states of vigilance and mentation. Neuroscience. 101:243–276.

Steriade M. 2006. Grouping of brain rhythms in corticothalamic systems. Neuroscience. 137:1087–1106.

Takada M, Tokuno H, Hamada I, Inase M, Ito Y, Imanishi M, Hasegawa N, Akazawa T, Hatanaka N, Nambu A. 2001. Organization of inputs from cingulate motor areas to basal ganglia in macaque monkey. Eur J Neurosci. 14:1633–1650.

Tallon-Baudry C, Bertrand O. 1999. Oscillatory gamma activity in humans and its role in object representation. Trends Cogn Sci. 3:151–162.

Tallon-Baudry C, Bertrand O, Delpuech C, Pernier J. 1996. Stimulus specificity of phase-locked and non-phase-locked 40 Hz visual responses in human. J Neurosci. 16:4240–4249.

Tanji J, Mushiake H. 1996. Comparison of neuronal activity in the supplementary motor area and primary motor cortex. Brain Res Cogn Brain Res. 3:143–150.

Tseng KY, Kasanetz F, Kargieman L, Riquelme LA, Murer MG. 2001. Cortical slow oscillatory activity is reflected in the membrane potential and spike trains of striatal neurons in rats with chronic nigrostriatal lesions. J Neurosci. 21:6430–6439.

Turner RS, Anderson ME. 2005. Context-dependent modulation of movement-related discharge in the primate globus pallidus. J Neurosci. 25:2965–2976.

Uhlhaas PJ, Singer W. 2006. Neural synchrony in brain disorders: relevance for cognitive dysfunctions and pathophysiology. Neuron. 52:155–168.

Urbain N, Gervasoni D, Souliere F, Lobo L, Rentero N, Windels F, Astier B, Savasta M, Fort P, Renaud B, et al. 2000. Unrelated course of subthalamic nucleus and globus pallidus neuronal activities across vigilance states in the rat. Eur J Neurosci. 12:3361–3374.

Varela F, Lachaux J-P, Rodriguez E, Martinerie J. 2001. The brainweb: phase synchronization and large scale intergration. Nat Rev Neurosci. 2:229–239.

Walters JR, Hu D, Itoga CA, Parr-Brownlie LC, Bergstrom DA. 2007. Phase relationships support a role for coordinated activity in the indirect pathway in organizing slow oscillations in basal ganglia output after loss of dopamine. Neuroscience. 144:762–776.

Wichmann T, Bergman H, DeLong MR. 1994. The primate subthalamic nucleus I: Functional properties in intact animals. J Neurophysiol. 72:494–506.

Wichmann T, Kliem MA. 2004. Neuronal activity in the primate substantia nigra pars reticulata during the performance of simple and memory-guided elbow movements. J Neurophysiol. 91:815–827.

Wichmann T, DeLong MR. 2006. Deep brain stimulation for neurologic and neuropsychiatric disorders. Neuron. 52:197–204.

Wichmann T, Soares J. 2006. Neuronal firing before and after burst discharges in the monkey Basal Ganglia is predictably patterned in the normal state and altered in parkinsonism. J Neurophysiol. 95:2120–2133.

Williamson P. 2007. Are anticorrelated networks in the brain relevant to schizophrenia? Schizophr Bull. 33:994–1003.